Complementary optical rogue waves in parametric three-wave mixing

Shihua Chen,[1,*] Xian-Ming Cai,[1] Philippe Grelu,[2] J. M. Soto-Crespo,[3,5] Stefan Wabnitz,[4] and Fabio Baronio[4,6]

[1]*Department of Physics, Southeast University, Nanjing 211189, China*
[2]*Laboratoire Interdisciplinaire Carnot de Bourgogne, U.M.R. 6303 C.N.R.S., Université Bourgogne Franche-Comté, 9 Avenue A. Savary, F-21078 Dijon, France*
[3]*Instituto de Óptica, Consejo Superior de Investigaciones Científicas (CSIC), Serrano 121, Madrid 28006, Spain*
[4]*INO CNR and Dipartimento di Ingegneria dell'Informazione, Università di Brescia, Via Branze 38, 25123 Brescia, Italy*
[5]*jsoto@io.cfmac.csic.es*
[6]*fabio.baronio@unibs.it*
[*]*cshua@seu.edu.cn*

Abstract: We investigate the resonant interaction of two optical pulses of the same group velocity with a pump pulse of different velocity in a weakly dispersive quadratic medium and report on the complementary rogue wave dynamics which are unique to such a parametric three-wave mixing. Analytic rogue wave solutions up to the second order are explicitly presented and their robustness is confirmed by numerical simulations, in spite of the onset of modulation instability activated by quantum noise.

OCIS codes: (190.3100) Instabilities and chaos; (190.5530) Pulse propagation and temporal solitons; (190.4410) Nonlinear optics, parametric processes.

References and links

1. D. R. Solli, C. Ropers, P. Koonath, and B. Jalali, "Optical rogue waves," Nature (London) **450**, 1054–1057 (2007).
2. J. M. Dudley, G. Genty, and B. J. Eggleton, "Harnessing and control of optical rogue waves in supercontinuum generation," Opt. Express **16**(6), 3644–3651 (2008).
3. B. Kibler, J. Fatome, C. Finot, G. Millot, F. Dias, G. Genty, N. Akhmediev, and J. M. Dudley, "The Peregrine soliton in nonlinear fibre optics," Nature Phys. **6**, 790–795 (2010).
4. C. Lecaplain, Ph. Grelu, J. M. Soto-Crespo, and N. Akhmediev, "Dissipative rogue waves generated by chaotic pulse bunching in a mode-locked laser," Phys. Rev. Lett. **108**, 233901 (2012).
5. S. Birkholz, E. T. J. Nibbering, C. Bree, S. Skupin, A. Demircan, G. Genty, and G. Steinmeyer, "Spatiotemporal rogue events in optical multiple filamentation," Phys. Rev. Lett. **111**, 243903 (2013).
6. F. Selmi, S. Coulibaly, Z. Loghmari, I. Sagnes, G. Beaudoin, M. G. Clerc, and S. Barbay, "Spatiotemporal chaos induces extreme events in an extended microcavity laser," Phys. Rev. Lett. **116**, 013901 (2016).
7. N. Akhmediev, A. Ankiewicz, and M. Taki, "Waves that appear from nowhere and disappear without a trace," Phys. Lett. A **373**, 675–678 (2009).
8. M. Onorato, S. Residori, U. Bortolozzo, A. Montina, and F. T. Arecchi, "Rogue waves and their generating mechanisms in different physical contexts," Phys. Rep. **528**, 47–89 (2013).
9. N. Akhmediev, J. M. Dudley, D. R. Solli, and S. K. Turitsyn, "Recent progress in investigating optical rogue waves," J. Opt. **15**, 060201 (2013).
10. J. M. Dudley, F. Dias, M. Erkintalo, and G. Genty, "Instabilities, breathers and rogue waves in optics," Nature Photon. **8**, 755–764 (2014).
11. A. Chabchoub, N. P. Hoffmann, and N. Akhmediev, "Rogue wave observation in a water wave tank," Phys. Rev. Lett. **106**, 204502 (2011).
12. A. Chabchoub, B. Kibler, J. M. Dudley, and N. Akhmediev, " Hydrodynamics of periodic breathers," Phil. Trans. R. Soc. A **372**, 20140005 (2014).

#258969 Received 5 Feb 2016; revised 4 Mar 2016; accepted 6 Mar 2016; published 9 Mar 2016

13. D. J. Kaup, A. Reiman, and A. Bers, "Space-time evolution of nonlinear three-wave interactions. I. Interaction in a homogeneous medium," Rev. Mod. Phys. **51**, 275–309 (1979).
14. E. Ibragimov and A. Struthers, "Second-harmonic pulse compression in the soliton regime," Opt. Lett. **21**(19), 1582–1584 (1996).
15. A. Picozzi and M. Haelterman, "Parametric three-wave soliton generated from incoherent light," Phys. Rev. Lett. **86**, 2010–2013 (2001).
16. M. Conforti, F. Baronio, A. Degasperis, and S. Wabnitz, "Parametric frequency conversion of short optical pulses controlled by a CW background," Opt. Express **15**(19), 12246–12251 (2007).
17. A. Abdolvand, A. Nazarkin, A. V. Chugreev, C. F. Kaminski, and P. St. J. Russell, "Solitary pulse generation by backward Raman scattering in H_2-filled photonic crystal fibers," Phys. Rev. Lett. **103**, 183902 (2009).
18. E. Picholle, C. Montes, C. Leycuras, O. Legrand, and J. Botineau, "Observation of dissipative superluminous solitons in a Brillouin fiber ring laser," Phys. Rev. Lett. **66**, 1454–1457 (1991).
19. V. M. Malkin, G. Shvets, and N. J. Fisch, "Fast compression of laser beams to highly overcritical powers," Phys. Rev. Lett. **82**, 4448–4451 (1999).
20. M. Conforti, F. Baronio, A. Degasperis, and S. Wabnitz, "Inelastic scattering and interactions of three-wave parametric solitons," Phys. Rev. E **74**, 065602(R) (2006).
21. F. Baronio, M. Conforti, C. De Angelis, A. Degasperis, M. Andreana, V. Couderc, and A. Barthélémy, "Velocity-locked solitary waves in quadratic media," Phys. Rev. Lett. **104**, 113902 (2010).
22. F. Baronio, M. Conforti, A. Degasperis, and S. Lombardo, "Rogue waves emerging from the resonant interaction of three waves," Phys. Rev. Lett. **111**, 114101 (2013).
23. A. Degasperis and S. Lombardo, "Rational solitons of wave resonant-interaction models," Phys. Rev. E **88**, 052914 (2013).
24. S. Chen, J. M. Soto-Crespo, and Ph. Grelu, "Watch-hand-like optical rogue waves in three-wave interactions," Opt. Express **23**(1), 349–359 (2015).
25. S. Chen, F. Baronio, J. M. Soto-Crespo, Ph. Grelu, M. Conforti, and S. Wabnitz, "Optical rogue waves in parametric three-wave mixing and coherent stimulated scattering," Phys. Rev. A **92**, 033847 (2015).
26. F. Baronio, M. Conforti, A. Degasperis, S. Lombardo, M. Onorato, and S. Wabnitz, "Vector rogue waves and baseband modulation instability in the defocusing regime," Phys. Rev. Lett. **113**, 034101 (2014).
27. F. Baronio, S. Chen, Ph. Grelu, S. Wabnitz, and M. Conforti, "Baseband modulation instability as the origin of rogue waves," Phys. Rev. A **91**, 033804 (2015).
28. S. Chen, Ph. Grelu, and J. M. Soto-Crespo, "Dark- and bright-rogue-wave solutions for media with long-wave–short-wave resonance," Phys. Rev. E **89**, 011201(R) (2014).
29. S. Chen, J. M. Soto-Crespo, and Ph. Grelu, "Coexisting rogue waves within the (2+1)-component long-wave–short-wave resonance," Phys. Rev. E **90**, 033203 (2014).
30. F. Baronio, A. Degasperis, M. Conforti, and S. Wabnitz, "Solutions of the vector nonlinear Schrödinger equations: Evidence for deterministic rogue waves," Phys. Rev. Lett. **109**, 044102 (2012).
31. S. Chen, J. M. Soto-Crespo, and Ph. Grelu, "Dark three-sister rogue waves in normally dispersive optical fibers with random birefringence," Opt. Express **22**(22), 27632–27642 (2014).
32. L.-C. Zhao and J. Liu, "Rogue-wave solutions of a three-component coupled nonlinear Schrödinger equation," Phys. Rev. E **87**, 013201 (2013).
33. A. Ankiewicz, D. J. Kedziora, and N. Akhmediev, "Rogue wave triplets," Phys. Lett. A **375**, 2782–2785 (2011).
34. A. Chabchoub and N. Akhmediev, "Observation of rogue wave triplets in water waves," Phys. Lett. A **377**, 2590–2593 (2013).
35. M. Onorato, A. R. Osborne, and M. Serio, "Modulational instability in crossing sea states: A possible mechanism for the formation of freak waves," Phys. Rev. Lett. **96**, 014503 (2006).
36. S. Wabnitz and B. Wetzel, "Instability and noise-induced thermalization of Fermi–Pasta–Ulam recurrence in the nonlinear Schrödinger equation," Phys. Lett. A **378**, 2750–2756 (2014).
37. S. Toenger, T. Godin, C. Billet, F. Dias, M. Erkintalo, G. Genty, and J. M. Dudley, "Emergent rogue wave structures and statistics in spontaneous modulation instability," Sci. Rep. **5**, 10380 (2015).
38. B. Frisquet, B. Kibler, Ph. Morin, F. Baronio, M. Conforti, G. Millot, and S. Wabnitz, "Optical dark rogue wave," Sci. Rep. **6**, 20785 (2016).
39. K. Goda and B. Jalali, "Dispersive Fourier transformation for fast continuous single-shot measurements," Nature Photon. **7**, 102–112 (2013).
40. P. St. J. Russell, D. Culverhouse, and F. Farahi, "Theory of forward stimulated Brillouin scattering in dual-mode single-core fibers," IEEE J. Quantum Electron. **27**, 836–842 (1991).

1. Introduction

Recently there has been a surge of significant research activities on rare optical events [1–6] that are the optical equivalent of oceanic rogue waves, the latter being elusive and intrinsically hard to monitor due to the risky observational conditions [7, 8]. Optical rogue waves are

#258969 Received 5 Feb 2016; revised 4 Mar 2016; accepted 6 Mar 2016; published 9 Mar 2016

now known to possess the hallmark characteristics of oceanic rogue waves (*e.g.*, seemingly unpredictable with fantastic amplitude, transient and temporally steep, and following a skewed *L*-shaped statistics), but provide a more convenient pathway through which a deep understanding of those otherwise mysterious freaks of the sea is possible, thanks to the rapid progress in material engineering and the availability of sampling and diagnostic technology for ultrafast optics [9, 10]. Like their hydrodynamic counterparts [11, 12], optical rogue waves have become the fascinating arena for studying and unveiling the origin of different extreme wave dynamics that can be shared by diverse physical branches, *e.g.*, oceanography, plasma physics, nonlinear optics, and Bose-Einstein condensation [9, 10].

Three-wave mixing is among the most important fundamental processes in nonlinear optics that occurs in any weakly dispersive medium whose lowest-order nonlinearity is quadratic in terms of the wave amplitudes [13]. It usually describes parametric processes such as second-harmonic generation, parametric amplification or oscillation, and frequency conversion [14–16], whereas when extended to nonparametric scenarios, it can apply as well to the transient stimulated Raman scattering [17], stimulated Brillouin scattering [18], and even the laser-plasma interaction [19]. As early as 1970s, integrability of the governing equation, also known as three-wave resonant interaction (TWRI) equation, was established and soliton solutions were identified [13]. These TWRI solitons are coherent localized structures that result from a dynamic balance between the energy exchange due to the nonlinear interaction and the convection due to the group-velocity mismatch. They are able to propagate with a common velocity, despite the fact that the three waves travel with different group velocities before they are mutually trapped [20, 21]. This property makes such solitons very alluring for potential applications, since the walk-off caused by group-velocity mismatch, which usually limits the frequency conversion efficiency, can be circumvented by nonlinear coupling.

More interestingly, in addition to the velocity-locked solitons, the TWRI equation also admits families of spatiotemporally localized structures on a finite background—rogue waves [22, 23]. These exotic rogue wave structures can model the sudden appearance of amplitude peaks in a basic multicomponent nonlinear wave system, whose dynamics is beyond the reach of the scalar nonlinear Schrödinger (NLS) equation framework. Also, the intriguing dynamics of watch-hand-like super-rogue waves were demonstrated to occur in a parametric three-wave mixing process [24]. These super-rogue waves exhibit a relative robustness against white noise perturbations together with a non-overlapping distribution property, hence facilitating the forthcoming experimental observation and diagnostics. Most recently, the rogue wave dynamics in coherent stimulated scattering were also revealed [25], exhibiting markedly different dark-dark-bright patterns as well as a finite existence regime that coincides with the regime given by the baseband modulation instability (MI) theory [26, 27].

In this article, we investigate the nontrivial limiting case of a general three-wave mixing process that was not penetratingly explored before and report on the novel complementary rogue wave dynamics unique to this special parametric process. To put it differently, we find that the two rogue wave components having the same group velocity will be spatiotemporally balanced in intensity distribution, independently of what complex patterns the rogue waves will exhibit and whether or not their background heights are equal. This is distinctly different from the typical rogue wave dynamics occurring in two- or three-wave resonant media [28, 29] or in the two- or three-component Manakov systems [30–32]. We provide general exact analytic solutions for these complementary rogue waves as well as numerical evidences for their robustness in spite of the onset of MI activated by quantum noise.

#258969 Received 5 Feb 2016; revised 4 Mar 2016; accepted 6 Mar 2016; published 9 Mar 2016

2. Fundamental and the second-order rogue wave solutions

The TWRI equation that governs the resonant interaction of two optical pulses of the same group velocity ($V_2 = V_1 = V$) with a pump pulse of slower/higher velocity V_3, perfectly phase-matched in a weakly dispersive quadratic medium, can be written as [13, 20, 22]

$$u_{1t} + Vu_{1x} = u_2^* u_3^*, \quad u_{2t} + Vu_{2x} = -u_1^* u_3^*, \quad u_{3t} + V_3 u_{3x} = u_1^* u_2^*, \tag{1}$$

where $u_n(x,t)$ $(n = 1,2,3)$ are slowly varying complex envelopes of the three optical fields, with t and x being the time and space variables, respectively. In what follows, we assume $V_3 = 0$, which implies writing Eqs. (1) in a reference frame comoving with the field u_3. The subscripts stand for the partial derivatives and the asterisk denotes the complex conjugation. We emphasize that the above choice of signs before quadratic terms is indicative of the nonexplosive character of the interaction which can admit localized solutions [13].

Considering the resonant conditions for the frequencies and momenta, Eqs. (1) allow the following coupled plane-wave solutions

$$\begin{aligned} u_{10}(x,t) &= a_1 \exp\left[-i(k_1 x - \omega_1 t)\right], \\ u_{20}(x,t) &= a_2 \exp\left[i(k_2 x - \omega_2 t)\right], \\ u_{30}(x,t) &= ia_3 \exp\left[i(k_1 - k_2)x - i(\omega_1 - \omega_2)t\right], \end{aligned} \tag{2}$$

where

$$a_3 = \frac{a_1 a_2}{\delta}, \quad k_1 = \frac{\omega_1}{V} + \frac{a_2^2}{\delta V}, \quad k_2 = \frac{\omega_2}{V} + \frac{a_1^2}{\delta V}, \tag{3}$$

with a_n being the respective background heights. For the sake of convenience, we use $A = a_1^2 + a_2^2$, $B = a_1^2 - a_2^2$, $\kappa = \omega_1 + \omega_2$, and $\delta = \omega_1 - \omega_2$. In this paper, we always assume $\omega_1 > \omega_2$, i.e., $\delta > 0$, without loss of generality. As indicated in [25], such background fields are intrinsically unstable and can evolve into the rogue wave or breather structures.

We noted that Eqs. (1) correspond to the limiting or degenerate case of those shown in [25], so are their rogue wave solutions. Hence, based on those known nondegenerate solutions, we take the limit $V_2 \to V_1 = V$ and obtain the exact fundamental rogue wave solutions

$$\begin{aligned} u_1^{[1]} &= u_{10}\left\{1 + \frac{2i\delta V[\delta^2 Vt - (\delta^2 + A)x] - \delta^2 AV^2/a_1^2}{[\delta^2 Vt - (\delta^2 + B)x]^2 + 4\delta^2 a_3^2 x^2 + A^2V^2/(4a_3^2)}\right\}, \\ u_2^{[1]} &= u_{20}\left\{1 + \frac{2i\delta V[\delta^2 Vt - (\delta^2 - A)x] - \delta^2 AV^2/a_2^2}{[\delta^2 Vt - (\delta^2 + B)x]^2 + 4\delta^2 a_3^2 x^2 + A^2V^2/(4a_3^2)}\right\}, \\ u_3^{[1]} &= u_{30}\left\{1 - \frac{4i\delta^3 V(Vt - x) + A^2V^2/a_3^2}{[\delta^2 Vt - (\delta^2 + B)x]^2 + 4\delta^2 a_3^2 x^2 + A^2V^2/(4a_3^2)}\right\}. \end{aligned} \tag{4}$$

Noteworthily, the above fundamental rogue wave solutions generalize the solutions (32) in [25], by lifting any constraints on the background heights a_1 and a_2. Further, the second-order rogue wave solutions of Eqs. (1) can be found in the same way, but need more complicated manipulations. These second-order solutions are given explicitly below:

$$\begin{aligned} u_1^{[2]} &= u_{10}\left\{1 - \frac{4ia_2 R_1^*[M_4(|R_2|^2 M_2^* - M_1) + R_0(|R_1|^2 M_2 + |R_2|^2 M_2^*)]}{\delta(M_1^2 + |R_1 R_2 M_2|^2)}\right\}, \\ u_2^{[2]} &= u_{20}\left\{1 - \frac{4ia_1 R_2[M_3^*(|R_1|^2 M_2 + M_1) + R_0^*(|R_1|^2 M_2 + |R_2|^2 M_2^*)]}{\delta(M_1^2 + |R_1 R_2 M_2|^2)}\right\}, \\ u_3^{[2]} &= u_{30}\left\{1 - \frac{4iR_1 R_2^*[|R_1|^2(2 + M_2^*) + |R_2|^2(2 - M_2)]}{M_1^2 + |R_1 R_2 M_2|^2}\right\}, \end{aligned} \tag{5}$$

#258969 Received 5 Feb 2016; revised 4 Mar 2016; accepted 6 Mar 2016; published 9 Mar 2016

where

$$R_0 = \gamma_1 + \gamma_2\xi, \quad R_j = \frac{a_j}{\alpha_j}(\gamma_1 + \gamma_2\theta_j), \text{ (here and below } j = 1,\ 2), \tag{6}$$

$$S_0 = -i\gamma_1\xi\varphi + \gamma_2[q\xi - 4ia_3x/(\delta V)] + \gamma_3 - i\gamma_4\xi, \tag{7}$$

$$S_j = \frac{\alpha_j S_0 + i\gamma_1\phi^2[\theta_j - A/(2\delta^2 a_3)] + \gamma_2(\phi^2\vartheta_j - iq) - \gamma_4}{\alpha_j(\gamma_1 + \gamma_2\theta_j)}, \tag{8}$$

$$\xi = t - \left[\frac{1}{V}\left(1 + \frac{B}{\delta^2}\right) + \frac{2ia_3}{\delta V}\right]x, \tag{9}$$

$$\alpha_j = \frac{\delta}{2A}[B - 2i\delta a_3 - (-1)^j A], \quad \theta_j = \xi - \frac{i}{\alpha_j}, \tag{10}$$

$$\vartheta_j = \frac{[\theta_j - 3A/(2\delta^2 a_3)](2 + i\alpha_j\xi)\alpha_j - i}{3\alpha_j^2}, \tag{11}$$

$$\phi = \frac{2\delta^2 a_3}{A^2}\sqrt{A^2 - 2B^2 + 4i\delta B a_3}, \quad \varphi = \frac{i\phi^2 A}{2\delta^2 a_3} + \frac{2ia_3(\delta^2 - A)}{3A}, \tag{12}$$

$$q = -i\xi\varphi + \frac{\phi^2}{3}\xi^2 - \frac{A^2\phi^2}{4\delta^4 a_3^2} - \frac{1}{2}, \tag{13}$$

$$M_1 = |R_1|^2 + |R_2|^2 > 0, \quad M_2 = S_2 - S_1, \tag{14}$$

$$M_3 = S_1R_0 - S_0 - 2R_0, \quad M_4 = S_2R_0 - S_0 - 2R_0. \tag{15}$$

Here γ_s ($s = 1,2,3,4$) are four arbitrary complex constants, which are responsible for all rogue wave structures of second hierarchy, for instance, the composite rogue waves, the rogue wave triplets [33,34], and their dark cousins. We need to point out that to form the second-order rogue wave hierarchy, γ_2 should not be vanishing, otherwise the solutions (5), after an appropriate translation along the t and x axes, can be reduced to the fundamental solutions (4). An inspection of Eqs. (4) and (5) reveals that the rogue wave structures do not depend on the frequency sum κ, which only appears in the propagation factor. For this reason, we always assume $\kappa = 0$ in our numerical examples given below, unless otherwise mentioned.

3. Novel complementary dynamics and discussions

Let us take a more exhaustive look into the structure of the most simple Peregrine rogue waves defined by Eqs. (4). It is shown that, while the rogue wave component u_3 possesses a peak amplitude fixedly three times its background height (significant wave height), the first two components u_1 and u_2 involve a peak amplitude varying with the relative magnitude of a_1 and a_2, given by $a_1|1 - 4a_2^2/A|$ and $a_2|1 - 4a_1^2/A|$, respectively. As examples, if $a_2 = a_1$, these two rogue waves will have the same height at the origin as in the far periphery, and thus feature an intermediate rogue wave structure, for which one can refer to Fig. 4 in [25] for details. However, if $a_2 = \sqrt{3}a_1$, while the field u_1 takes the bright structure peaking twice as high as the average background, the field u_2 will be a *black rogue wave* component whose intensity can fall to zero in the dip center. Of course, if $a_1 = \sqrt{3}a_2$, the opposite will be true. No matter what situation it is in, the third field u_3 always displays a usual Peregrine soliton structure.

The above conclusions can apply as well to the situation of higher-order rogue waves, by which one can determine whether they are bright or not. Nonetheless, there could be more to it. Considering the second-order rogue wave solutions (5), it is obvious that their dynamics are more complicated than what Peregrine solitons could exhibit, as they depend not only on the starting plane-wave parameters, but also on four structural parameters γ_s. To be specific, the parameter γ_2, if nonvanishing, gives rise to a rogue wave skeleton of second order, on which

#258969 Received 5 Feb 2016; revised 4 Mar 2016; accepted 6 Mar 2016; published 9 Mar 2016

the spatiotemporal distribution of patterns could be influenced remarkably by the other three structural parameters. For instance, an increase of the value of any of these three parameters at given γ_2 will enable the second-order rogue wave to evolve into a triplet pattern which consists of three fundamental rogue waves [25, 31, 33].

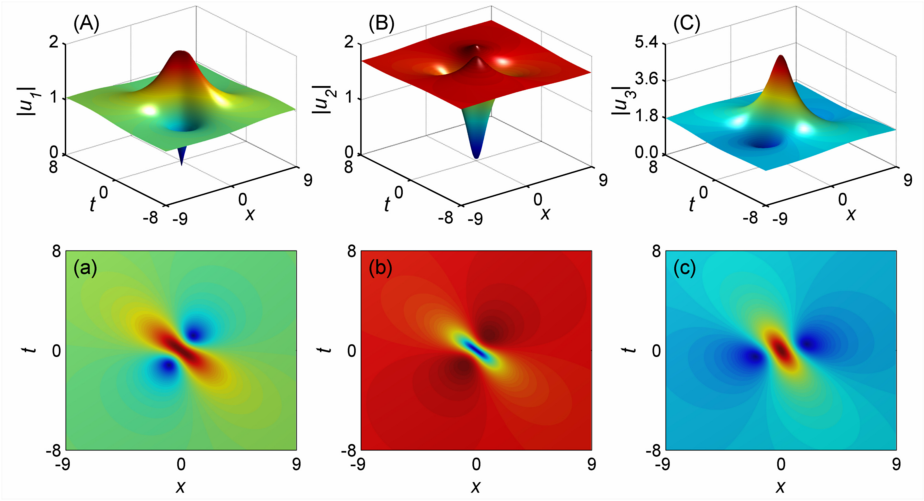

Fig. 1. Fundamental optical rogue waves formed at $a_1 = 1$, $a_2 = a_3 = \sqrt{3}$, $\delta = 1$, and $V = 4$. (A)–(C) surface plots; (a)–(c) the corresponding contour distributions.

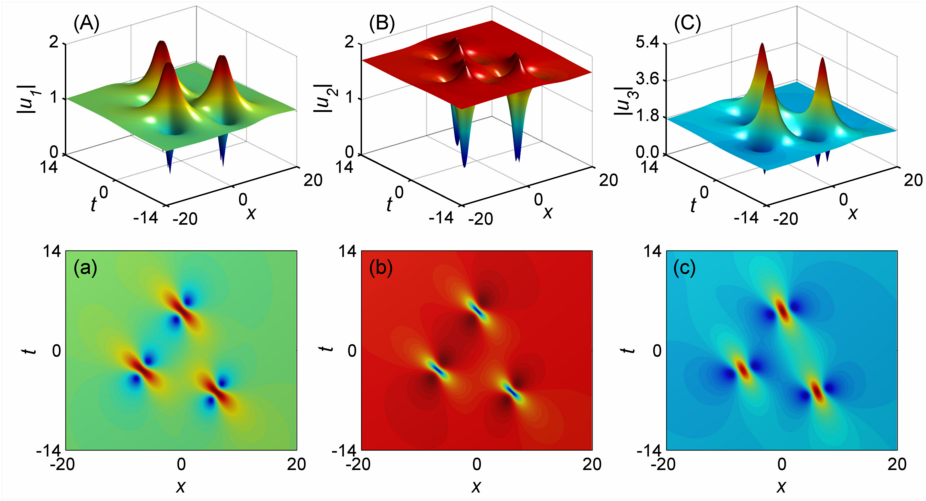

Fig. 2. Rogue wave triplets formed under the same initial plane-wave parameters as in Fig. 1, but with extra structural parameters given by $\gamma_1 = 7$, $\gamma_2 = 1$, and $\gamma_3 = \gamma_4 = 0$. (A)–(C) surface plots; (a)–(c) the corresponding contour distributions.

More interestingly, it is revealed that the sum of the intensities of the components u_1 and u_2 will always be conserved and can be given by

$$|u_1|^2 + |u_2|^2 = a_1^2 + a_2^2 = A, \tag{16}$$

#258969 Received 5 Feb 2016; revised 4 Mar 2016; accepted 6 Mar 2016; published 9 Mar 2016

independently of what parameters γ_s we choose for deterministic rogue wave structures and whether or not their background heights are equal. As a matter of fact, the relation (16) is a natural consequence of Eqs. (1) which suggest that $(\frac{\partial}{\partial t}+V\frac{\partial}{\partial x})(|u_1|^2+|u_2|^2)=0$. Therefore, if the field u_1 takes a bright Peregrine [3] or a bright triplet [33] structure, the field u_2 will take the corresponding dark counterpart so that Eq. (16) can be fulfilled. In other words, they are spatiotemporally complementary, hence the name *complementary rogue waves*.

Figures 1 and 2 illustrate the complementary dynamics of typical Peregrine-like rogue waves [see 1(A)–1(C)] and of the rogue wave triplets [see 2(A)–2(C)], respectively, by choosing the same initial plane-wave parameters for both situations and an extra set of structural parameters for the latter situation, all of which have been specified in the captions. It is clear that the three fields u_n would take the bright, black, and bright structures, respectively, but the first two are always spatiotemporally balanced according to Eq. (16), independently of whether the three rogue wave components are Peregrine-like (see Fig. 1) or are of triplet pattern (see Fig. 2).

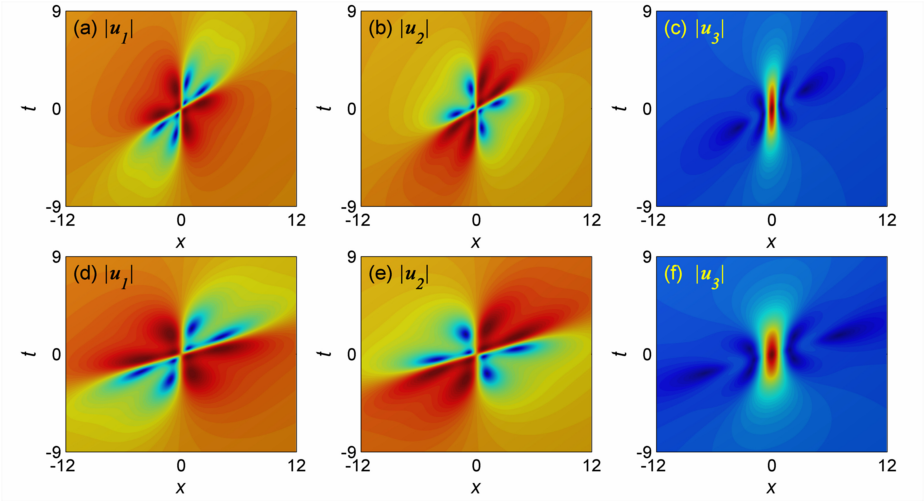

Fig. 3. Second-order optical rogue waves formed at $a_1=a_2=a_3=1$, and $\delta=1$, for given structural parameters $\gamma_1=-0.5$, $\gamma_2=1$, and $\gamma_3=\gamma_4=0$. (a)–(c) $V=2$; (d)–(f) $V=4$. (a), (b), (d), and (e) show a butterfly-type pattern, while (c) and (f) show a bright structure.

A further study suggests that the role of the parameter V played in the complementary dynamics is simple and is just to expand (contract) the spatiotemporal pattern along the x axis as V increases (decreases). This is not surprising because the parameter V in Eqs. (1) takes the part of a "width" in the x direction and indeed can be removed by a change of variables. For illustration, we show in Fig. 3 the evolution dynamics of the second-order rogue waves with the same background height (see captions for specific parameter values). It is easily seen that the former two butterfly-type patterns are markedly expanded along the x axis if the value of V increases from 2 [see 3(a) and 3(b)] to 4 [see 3(d) and 3(e)], while keeping spatiotemporally complementary all through the evolution. So is the case with the third rogue wave component u_3 which, however, is always bright, as seen in Figs. 3(c) and 3(f).

4. MI and numerical simulations

It is easily concluded from Eqs. (4) and (5) that the complementary rogue waves can exist in the whole parametric space. As a matter of fact, one can verify this using the recently-proposed

#258969 Received 5 Feb 2016; revised 4 Mar 2016; accepted 6 Mar 2016; published 9 Mar 2016

baseband MI theory for rogue waves [26, 27], which equates the existence regime of rogue waves with that of nonzero MI gain at arbitrarily low modulation frequency. This can be done by calculating the MI of the background fields that support the formation of rogue waves [35]. To this end, we add small-amplitude Fourier modes to the plane-wave solutions (2), and express them as $u_n = u_{n0}\{1 + p_n \exp[-i\Omega(\mu t - x)] + q_n^* \exp[i\Omega(\mu^* t - x)]\}$ $(n = 1, 2, 3)$, where p_n and q_n are small amplitudes of the Fourier modes, and the parameters Ω and μ are assumed to be positive and complex, respectively [24, 25, 27]. A substitution of these perturbed plane-wave solutions into Eqs. (1) followed by linearization yields the dispersion relation

$$\Omega^2\mu^2 - \frac{4\mu a_1^2}{\mu - V} - \left[\frac{\mu A}{\delta(\mu - V)} - \delta\right]^2 = 0. \tag{17}$$

Obviously, in the limit of $\Omega = 0$ (i.e., at an arbitrarily low modulation frequency in the baseband MI [26, 27]), Eq. (17) always permits a pair of complex conjugate roots in the whole regime of δ (of course excluding $\delta = 0$), confirming our analytic predictions mentioned above.

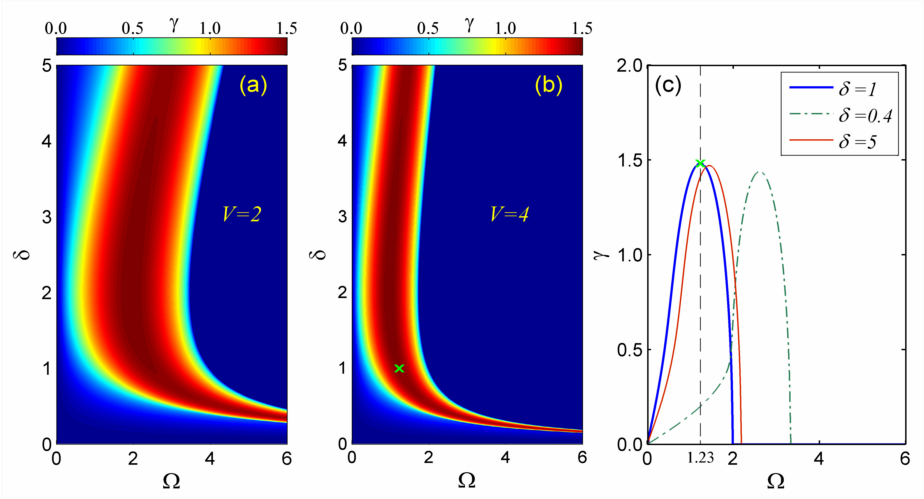

Fig. 4. Map of the MI gain versus Ω and δ for $a_1 = 1$ and $a_2 = \sqrt{3}$: (a) $V = 2$; (b) $V = 4$. (c) illustrates profiles of the growth rate γ versus Ω in (b) for several given values of δ. The same green cross in (b) and (c) indicates the maximum of the growth rate for given $\delta = 1$, which occurs at a modulation frequency of about 1.23.

Quartic equation (17) can indeed be exactly solved at an analytic level and hence the growth rate of the MI, defined by $\gamma = \Omega|\mathrm{Im}(\mu)|$, can be readily calculated. Figure 4 shows the MI gain map in the plane $(\Omega,\ \delta)$ for specific parameters $a_1 = 1$ and $a_2 = \sqrt{3}$. It is clear that the baseband MI could extend over the whole range of δ, since the passband MI that occurs in coherent stimulated backscattering (refer to Fig. 8 in Ref. [25]) is absent now, as revealed by Eq. (17). Moreover, as V increases from 2 [see panel (a)] to 4 [see panel (b)], the MI map contracts significantly, but with the maximum value of gain still unchanged. The latter may suggest that the MI-induced periodic waves possess fewer wave crests or troughs at $V = 4$ than at $V = 2$. In particular, for given initial parameters as in Fig. 1, the maximum of the growth rate γ will occur at the modulation frequency $\Omega \simeq 1.23$ [see the green cross in panel (c)].

Further, we performed extensive numerical simulations to study the evolution dynamics of complementary rogue waves, based on the standard split-step Fourier method [24, 25, 29]. Practically, of most concern to general soliton community is the stability of these rogue waves with

#258969 Received 5 Feb 2016; revised 4 Mar 2016; accepted 6 Mar 2016; published 9 Mar 2016

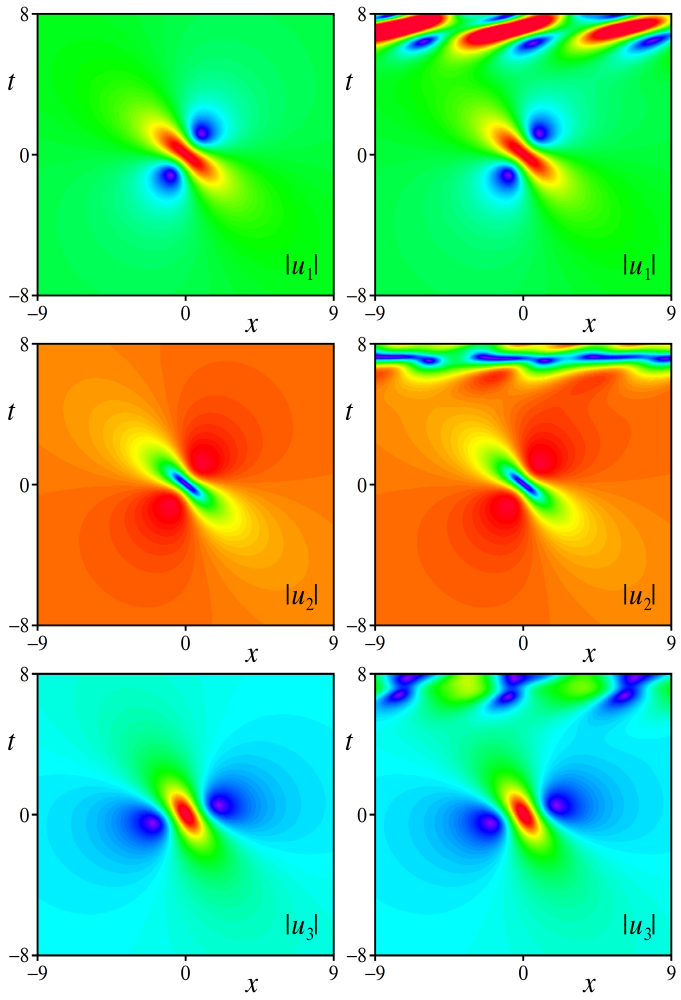

Fig. 5. Simulation results intended for the fundamental rogue waves using the same initial plane-wave parameters as in Fig. 1. Left column: unperturbed; Right column: perturbed by a white noise of the intensity $\varepsilon = 10^{-8}$.

respect to background broadband noise sources (*e.g.*, quantum noise) [36, 37]. In fact, recent work showed that the Fermi-Pasta-Ulam recurrence of Akhmediev breather solutions of the scalar NLS equation may eventually break down in the presence of competing spontaneous noise-activated MI [36]. For this purpose, we perturbed the initial deterministic rogue wave profiles by small amounts of white noise, and inspected whether the rogue wave generation is still observed in the presence of the MI activated by such quantum noise.

As in [24, 25], we multiplied the real and imaginary parts of all three field components u_n at sufficient negative times by a factor $[1+\varepsilon r_i(x)]$ $(i = 1, \ldots, 6)$, respectively, where r_i are six uncorrelated random functions uniformly distributed in the interval $[-1,\ 1]$ and ε is a small parameter defining the noise level. Figure 5 shows the numerical results intended for the fundamental rogue waves, either unperturbed (i.e., letting $\varepsilon = 0$) or perturbed by a small amount of white noise for which we choose $\varepsilon = 10^{-8}$. It is clear that without any perturbations (see left

#258969 Received 5 Feb 2016; revised 4 Mar 2016; accepted 6 Mar 2016; published 9 Mar 2016

column), our numerical simulations produce almost identical results as shown in Figs. 1(a)–1(c), hence giving evidence that the RW solution is robust against numerical integration noise accumulation. On the other hand, in the right column, we showed that all three rogue wave components, under tiny perturbations, can still propagate very neatly for a rather long time, till eventually the MI of background fields grows up. Moreover, one can infer from the first figure in the right column that the period of the MI-induced periodic wave is around $18/3.5$, corresponding to a modulation frequency of $7\pi/18 \simeq 1.22$, almost the same as calculated from our MI analysis, which has been indicated by the green cross in Fig. 4(c). Obviously, this good consistency confirms again the soundness of our numerical results.

Finally, we would like to suggest an experimental setup in the context of nonlinear optics for observation of such complementary rogue waves. In fact, nonlinear optics has recently unveiled deterministic bright [3] and dark [38] rogue waves. For the current issue under consideration, we may launch three phase-matched carrier waves of about 10-ps pulse duration, which can mimic quasi-continuous wave signals, in a periodically poled lithium niobate (PPLN) crystal of appropriate poling period to trigger a temporal type-II second harmonic interaction where u_1 and u_2 share the same group velocity. With this experimental setup and by virtue of fast pulse measuring techniques [39], we anticipate that MI evidence and the related complementary rogue wave dynamics could be observed with peak field intensities of hundreds $\mathrm{MW/cm^2}$.

There is also a possibility to realize complementary rogue waves in a dual-mode optical fiber where a forward stimulated Brillouin scattering can occur [40]. In this case, the group velocity of the pump and Stokes optical waves can be nearly identical, while in comparison, the velocity of the acoustic wave is close to zero, resulting in an intermodal coupling governed by Eqs. (1). Under these circumstances, the complementary rogue wave dynamics would occur and one could observe in optical fibers two-color optical rogue waves of bright-dark type, thanks to the coupling with the acoustic wave and the relatively long interaction length.

5. Conclusions

In conclusion, we studied the resonant interaction of two optical pulses of the same group velocity with a pump pulse of different velocity in a weakly dispersive quadratic medium. Novel complementary rogue wave dynamics were unveiled for such a special parametric three-wave mixing, based on the exact explicit analytic solutions up to the second order. Numerical simulations confirmed that these complementary rogue waves are stable enough to develop, in spite of the onset of MI activated by quantum noise. It foreshadows the possibility to observe such unique rogue wave phenomena in quadratic crystals or other nonparametric processes that can be governed by Eqs. (1). In this prospect, we proposed a realistic experimental frame for demonstration of such complementary rogue wave dynamics.

Acknowledgments

This work was supported by the National Natural Science Foundation of China (Grants No. 11174050 and No. 11474051) and by the Italian Ministry of University and Research (MIUR, Project No. 2012BFNWZ2). Ph. G. was supported by the Agence Nationale de la Recherche (Project No. ANR-2012-BS04-0011). The work of J. M. S. C. was supported by MINECO under contract TEC2012-37958-C02-02, by C.A.M. under contract S2013/MIT-2790, and by the Volkswagen Foundation.

#258969 Received 5 Feb 2016; revised 4 Mar 2016; accepted 6 Mar 2016; published 9 Mar 2016